Energy Efficiency Maximization via Joint Active and Passive Beamforming Design for Multiuser MISO IRS-Aided SWIPT

Shayan Zargari, Ata Khalili, *Graduate Student Member, IEEE*, and Rui Zhang, *Fellow, IEEE*

***Abstract*—This letter studies a multiuser multiple-input single-output (MISO) intelligent reflecting surface (IRS)-aided simultaneous wireless information and power transfer (SWIPT) system. Specifically, a multi-antenna base station (BS) transmits data along with energy to a set of users to decode data and harvest energy by adopting the power splitting (PS) simultaneously. The energy efficiency indicator (EEI) is introduced to trade off between data rate and harvested energy, which is maximized by jointly optimizing beamforming vectors at the BS, PS ratio at each user, and phase shifts at the IRS. To solve this non-convex optimization problem, we first adopt the majorization-minimization (MM) approach to construct a concave-convex fractional function which can be handled via the Dinkelbach algorithm and then propose an efficient algorithm for solving two subproblems based on the alternating optimization (AO). For the first subproblem, semi-definite relaxation (SDR), MM approach, and Dinkelbach algorithm are adopted, while for the second sub-problem, a new manifold approach is proposed to handle the unit-modulus constraints due to IRS passive reflection. Simulation results demonstrate the superior performance of our proposed algorithm compared to other baseline schemes.**

***Index Terms*—Intelligent reflecting surface, simultaneous wireless information and power transfer, energy efficiency.**

I. Introduction

INTELLIGENT reflecting surface (IRS) has lately drawn significant attention and growing interests as a promising technology for the sixth-generation (6G) wireless networks [1], [2]. The IRS can reflect signals toward a desirable receiver by controlling phase shifts to enhance the rate/reliability of wireless communication systems. Since the IRS operates in full-duplex mode and requires low power consumption, it is a candidate solution to improve the energy efficiency (EE) and spectral efficiency (SE). There are a plethora of works that have studied the performance of IRS-assisted wireless communication systems with the joint design of passive/active beamforming vector (PBV/ABV) at the IRS and the base station (BS), respectively (see, e.g., [3]–[6]). For example, a multi-IRS scenario was studied in [5], where the on-off state of each element at the IRS was optimized to maximize the EE of the network. In [6], the weighted sum-rate (WSR) of multiple users was maximized by joint optimizing the ABV and PBV under perfect and imperfect channel state information (CSI).

Simultaneous wireless information and power transfer (SWIPT) has drawn considerable attention in recent years to deliver energy and data simultaneously for a variety of scenarios such as the Internet of Things (IoT) with low-power devices [7]. For SWIPT systems, improving the communication rate/range, energy transmission efficiency, balancing information decoding (ID) and energy harvesting (EH) at each receiver, are challenging issues that need to be addressed [8]. Several works in the literature have investigated IRS-aided SWIPT systems [9]–[10]. For instance, the authors in [9] studied the weighted sum-power maximization problem such that the wireless coverage and the battery life of devices are extended. The authors in [10] minimized the total transmit power by proposing a penalty-based algorithm. The WSR of all users in an IRS-assisted SWIPT system with separate ID and EH receivers was investigated in [11].

Motivated by the research progress for IRS, it is envisioned that the IRS will be a promising technology to tackle the above challenges in SWIPT systems. However, the problem of jointly designing reflection/transmission to balance the performance tradeoff between the energy/data at each receiver, to our best knowledge, has not been appropriately addressed in the literature yet. This thus motivates us to study the EE tradeoff between data transmission and energy transfer in this work.

In this letter, a multiuser MISO IRS-aided SWIPT system based on the power splitting (PS) approach is studied. We consider a multi-antenna BS that transmits signals to a set of users by applying ABVs aided by an IRS via tuning its PBV. It is noted that this letter differs from the above works that considered separated ID receivers (IDRs) and EH receivers (EHRs), while in this letter, each receiver consists of both an IDR and an EHR. We jointly design the ABVs at the BS, the PBV at the IRS, and PS ratio at each user, to maximize the system energy efficiency indicator (EEI), which balances the EE for information and energy transmissions, subject to the maximum transmit power budget of the BS. This problem is non-convex and thus hard to solve. To cope with it, we propose an efficient algorithm based on the semi-definite relaxation (SDR), majorization-minimization (MM), alternating optimization (AO), and Dinkelbackh techniques. Besides, we optimize ABVs and PS ratios jointly for the first subproblem via a customized approximation and propose a new manifold optimization approach to design the PBV at the IRS subject to their unit-modulus constraints for the second subproblem. Simulation results reveal that our proposed algorithm can achieve considerable performance gains over the benchmark schemes.

Manuscript received October 13, 2020; revised November 6, 2020; accepted November 8, 2020. Date of publication November 16, 2020; date of current version March 9, 2021. This work was supported by NUS Research under Grant R-263-000-D12-114. The associate editor coordinating the review of this article and approving it for publication was C. Shen. *(Corresponding author: Rui Zhang.)*

Shayan Zargari is with the School of Electrical Engineering, Iran University of Science and Technology, Tehran 1684613114, Iran (e-mail: shayanzargari66@gmail.com).

Ata Khalili is with the Electronics Research Institute, Sharif University of Technology, Tehran 14115-111, Iran, and also with the Department of Electrical and Computer Engineering, Tarbiat Modares University, Tehran 14155, Iran (e-mail: ata.khalili@ieee.org).

Rui Zhang is with the Department of Electrical and Computer Engineering, National University of Singapore, Singapore 117583 (e-mail: elezhang@nus.edu.sg).

Digital Object Identifier 10.1109/LWC.2020.3037750

Notation: Vectors and matrices are expressed by boldface lower-case letters (e.g., $\mathbf{a}$) and capital letters (e.g., $\mathbf{A}$), respectively. For a square matrix $\mathbf{A}$, $\mathbf{A}^H$, $\mathbf{A}^T$, Tr($\mathbf{A}$), and Rank($\mathbf{A}$) are Hermitian conjugate transpose, transpose, trace, and rank of a matrix, respectively. $\mathbf{A} \succeq \mathbf{0}$ indicates a positive semidefinite matrix. $\mathrm{diag}(\cdot)$ is the diagonalization operation. unt($\mathbf{a}$) forms a vector whose elements are $\frac{a_1}{|a_1|}, \ldots, \frac{a_n}{|a_n|}$. The Euclidean norm of a complex vector, the real part of a complex number, and the absolute value of a complex scalar are denoted by $\|\cdot\|$, $\Re\{\}$, and $|\cdot|$, respectively. The expectation operator is denoted by $\mathbb{E}[\cdot]$, and $\mathbb{C}^{M\times N}$ represents $M \times N$ dimensional complex matrices. The distribution of a circularly symmetric complex Gaussian (CSCG) random vector with mean $\boldsymbol{\mu}$ and covariance matrix $\mathbf{C}$ is denoted by $\sim \mathcal{CN}(\boldsymbol{\mu}, \mathbf{C})$. Finally, $\circ$ denotes the Hadamard product between two matrices.

II. System Model

In this letter, a downlink MISO SWIPT system is considered with an M-antenna BS, an N-element IRS, and K single-antenna users in the set of $\mathcal{K} = \{1, \ldots, K\}$. It is assumed that the BS can acquire the CSI in the network that is needed for our proposed design by some practical means[1] (see [1] and references therein). The transmit signal at the BS can be represented as $\mathbf{s} = \sum_{k\in\mathcal{K}} \mathbf{v}_k x_k$, where x_k is the information symbol for user k assumed to be $x_k \sim \mathcal{CN}(0, 1),\ \forall k$. $\mathbf{v}_k \in \mathbb{C}^{M\times 1}$ denotes the transmit beam of user k. It is assumed that all channel links experience quasi-static flat fading. Denote the equivalent channel links between the IRS-to-user k, BS-to-IRS and BS-to-user k as $\mathbf{h}_{ru,k} \in \mathbb{C}^{N\times 1}$, $\mathbf{H} \in \mathbb{C}^{N\times M}$, and $\mathbf{h}_{bu,k} \in \mathbb{C}^{M\times 1}$, respectively. Define $\boldsymbol{\Theta} = \mathrm{diag}(\beta_1 e^{j\alpha_1},\ \beta_2 e^{j\alpha_2}, \ldots,\ \beta_N e^{j\alpha_N})$ as the reflection-coefficients matrix at the IRS. In particular, $\alpha_n \in (0, 2\pi]$ and $\beta_n \in [0, 1]$, $\forall n \in \{1, \ldots, N\}$ are the phase shift and reflection amplitude of the n-th component at the IRS, respectively. For ease of practical implementation [1], [2], we consider that the amplitudes of all components are equal to one i.e., $\beta_n = 1$, $\forall n$. The received signal at the k-th user is given by $y_k = \mathbf{h}_k^H \mathbf{s} + n_k$, where $n_k \sim \mathcal{CN}(0, \sigma_k^2)$ denotes the receiver noise with variance σ_k^2, and $\mathbf{h}_k^H \triangleq \mathbf{h}_{ru,k}^H \boldsymbol{\Theta} \mathbf{H} + \mathbf{h}_{bu,k}^H$ represents the equivalent channel link. The received signal at the user is further split into two streams by employing a PS structure with a weight of $1 - \rho_k$ and ρ_k for EH and ID, respectively. Note that the PS ratio is limited to $0 < \rho_k < 1$. Therefore, the received signal at the ID receiver can be written as $y_k^{\mathrm{ID}} = \sqrt{1-\rho_k}(\mathbf{h}_k^H \mathbf{s} + n_k) + z_k$, where $z_k \sim \mathcal{CN}(0, \delta_k^2)$ denotes the additional noise as a result of the signal processing at the ID receiver [8]. The signal-to-interference-plus-noise ratio (SINR) at user k can be written as

$$\mathrm{SINR}_k = \frac{\left|\mathbf{h}_k^H \mathbf{v}_k\right|^2}{\sum\limits_{i\in K, i\neq k} \left|\mathbf{h}_k^H \mathbf{v}_i\right|^2 + \sigma_k^2 + \frac{\delta_k^2}{1-\rho_k}},\ \forall k. \tag{1}$$

Moreover, the received signal at the EH section can be described as $y_k^{\mathrm{EH}} = \sqrt{\rho_k}(\mathbf{h}_k^H \mathbf{s} + n_k)$. Assume that the total harvested energy is linearly proportional to the received signal power at user k which is presented by $P_k = \eta_k \rho_k (\sum_{i\in\mathcal{K}} |\mathbf{h}_k^H \mathbf{v}_i|^2)$, where $\eta_k \in (0, 1]$ is the energy conversion efficiency. For conciseness, we define the feasible set of the design parameters as $(\rho_k, \mathbf{v}_k, \boldsymbol{\Theta}) \in \mathcal{H}$. In this letter, we consider the new metric of EEI for balancing the EE for information and energy transmissions in the SWIPT system, i.e., ($\frac{\sum_{k\in\mathcal{K}} \log_2(1+\mathrm{SINR}_k(\mathcal{H}))}{U_{TP}(\mathcal{H})}$ and $\frac{\sum_{k\in\mathcal{K}} P_k}{U_{TP}(\mathcal{H})}$), respectively, which is defined as

$$U_{\mathit{eff}}(\mathcal{H}) = \frac{\sum_{k\in\mathcal{K}} \log_2(1 + \mathrm{SINR}_k(\mathcal{H})) + \omega \sum_{k\in\mathcal{K}} P_k}{U_{TP}(\mathcal{H})}, \tag{2}$$

where ω is a predefined non-negative weight factor that controls the tradeoff and $U_{TP}(\mathcal{H}) = \sum_{k\in\mathcal{K}} ||\mathbf{v}_k||^2 + P_{\mathrm{Cir}} + P_{\mathrm{IRS}}$ is the total consumed power of the system. In addition, $P_{\mathrm{Cir}} = \sum_{k\in\mathcal{K}} p_k^{\mathrm{Cir}} + P_{\mathrm{BS}}^{\mathrm{Cir}}$ is a constant circuit power dissipation which includes power consumption of all electrical components in both the transmitter i.e., $P_{\mathrm{BS}}^{\mathrm{Cir}}$ and receivers i.e., p_k^{Cir}'s; while $P_{\mathrm{IRS}} = P_{\mathrm{Sta}} + MP_{\mathrm{Dyn}}$, where P_{Sta} and P_{Dyn} are the static power required to maintain the basic circuit operations of the IRS and the dynamic power per reflecting component, respectively.

III. Problem Formulation

In this section, we aim to maximize the EEI of the system by jointly designing of the PS ratios, ABVs at the BS, and PBV at the IRS. The considered problem can be mathematically formulated[2] as

$$(\mathrm{P1}):\ \underset{\rho_k, \mathbf{v}_k, \boldsymbol{\Theta}}{\text{maximize}}\ U_{\mathit{eff}}(\mathcal{H}) \tag{3a}$$

$$\text{s.t.}\ \sum_{k\in\mathcal{K}} \|\mathbf{v}_k\|^2 \leq p_{\max}, \tag{3b}$$

$$0 < \rho_k < 1,\ \forall k, \tag{3c}$$

$$|\boldsymbol{\Theta}_{nn}| = 1,\ \forall n, \tag{3d}$$

where constraint (3b) restricts the total available transmit power at the BS; (3c) expresses the PS ratio constraints; and (3d) guarantees that the diagonal phase shift matrix has N unit-modulus elements on its main diagonal.

IV. Proposed Solution

To solve problem (P1) efficiently, we employ the AO algorithm that decomposes the original problem into two subproblems. For the first sub-problem, the SDR technique and MM method are applied to jointly design the ABVs and PS ratios. Then, Dinkelbach method is used to transform its fractional form into an equivalent linear form. For the second subproblem, the manifold optimization approach is used to design the PBV at the IRS.

A. Joint Beamforming and PS Ratio Design With Fixed Phase Shifts

In this subsection, we consider IRS phase shifts, i.e., $\boldsymbol{\Theta}$ to be fixed. Then, (P1) can be handled efficiently by adopting the SDR technique. Let us define $\mathbf{V}_k = \mathbf{v}_k \mathbf{v}_k^H$ and $\mathbf{H}_k = \mathbf{h}_k \mathbf{h}_k^H$, $\forall k$. By denoting the set of feasible solutions

[1]The results in this letter serve as theoretical performance upper bounds for the SWIPT-IRS system with imperfect CSI in practice.

[2]Note that the considered problem formulation can be extended to the case with a minimum EH and/or data rate requirement.

as $(\rho_k, \mathbf{V}_k) \in \mathcal{Z}$, we have

$$(\mathrm{P2}): \quad \max_{\mathcal{Z}} \left\{ \frac{R(\mathcal{Z}) - S(\mathcal{Z}) + \omega\, Y(\mathcal{Z})}{G(\mathcal{Z})} \right\} \tag{4a}$$

$$\text{s.t.} \quad \sum_{k\in\mathcal{K}} \mathrm{Tr}(\mathbf{V}_k) \le p_{\max}, \tag{4b}$$

$$0 \le \rho_k \le 1, \ \forall k, \tag{4c}$$

$$\cancel{\mathrm{Rank}(\mathbf{V}_k) \le 1}, \quad \mathbf{V}_k \succeq \mathbf{0}, \ \forall k, \tag{4d}$$

where the rank-one constraint (4d) is dropped and

$$R(\mathcal{Z}) = \sum_{k\in\mathcal{K}} \log_2\Big(\sum_{i\in\mathcal{K}} \mathrm{Tr}(\mathbf{H}_k\mathbf{V}_i) + \sigma_k^2 + \frac{\delta_k^2}{1-\rho_k}\Big), \tag{5}$$

$$S(\mathcal{Z}) = \sum_{k\in\mathcal{K}} \log_2\Big(\sum_{i\in\mathcal{K}, i\neq k} \mathrm{Tr}(\mathbf{H}_k\mathbf{V}_i) + \sigma_k^2 + \frac{\delta_k^2}{1-\rho_k}\Big), \tag{6}$$

$$Y(\mathcal{Z}) = \sum_{k\in\mathcal{K}} \eta_k \sum_{i\in\mathcal{K}} X_i(\mathcal{Z}), \tag{7}$$

$$G(\mathcal{Z}) = \sum_{k\in\mathcal{K}} \mathrm{Tr}(\mathbf{V}_k) + P_{\mathrm{Cir}} + P_{\mathrm{IRS}}, \tag{8}$$

where $X_i(\mathcal{Z}) = \mathrm{Tr}(\rho_k \mathbf{H}_k \mathbf{V}_i)$. It is observed that the objective function in (P2) is not a concave one. However, the numerator in the objective function $(4\mathrm{a})$ belongs to the class of difference of two concave functions (DC). Since $S(\mathcal{Z})$ is a differentiable concave function, we have

$$S(\mathcal{Z}) \le S(\mathcal{Z}^{(t-1)}) + \sum_{k\in\mathcal{K}} \mathrm{Tr}\Big(\nabla_{\mathbf{V}_k}^H S(\mathcal{Z}^{(t-1)})(\mathbf{V}_k - \mathbf{V}_k^{(t-1)})\Big) + \sum_{k\in\mathcal{K}} \mathrm{Tr}\Big(\partial_{\rho_k} S(\mathcal{Z}^{(t-1)})\Big(\rho_k - \rho_k^{(t-1)}\Big)\Big) \triangleq \tilde{S}(\mathcal{Z}). \tag{9}$$

It is straight-forward to show that $X_i(\mathcal{Z})$ can be equivalently written as

$$X_i(\mathcal{Z}) = \tfrac{1}{2}\|\rho_k\mathbf{H}_k + \mathbf{V}_i\|_F^2 - \tfrac{\rho_k^2\,\mathrm{Tr}(\mathbf{H}_k{}^H\mathbf{H}_k)}{2} - \tfrac{\mathrm{Tr}(\mathbf{V}_i^H\mathbf{V}_i)}{2}. \tag{10}$$

However, (10) is still non-concave. To deal with it, we employ the MM approach via the first-order Taylor approximation as

$$F(\rho_k, \mathbf{V}_i) \triangleq \frac{1}{2}\|\rho_k\mathbf{H}_k + \mathbf{V}_i\|_F^2 \ge F(\rho_k^{(t)}, \mathbf{V}_i^{(t)}) + \mathrm{Tr}\Big(\partial_{\rho_k} F(\rho_k^{(t)}, \mathbf{V}_i^{(t)})(\rho_k - \rho_k^{(t)})\Big) + \mathrm{Tr}\Big(\nabla_{\mathbf{V}_i}^H F(\rho_k^{(t)}, \mathbf{V}_i^{(t)})(\mathbf{V}_i - \mathbf{V}_i^{(t)})\Big) \triangleq \tilde{F}(\rho_k, \mathbf{V}_i). \tag{11}$$

The proposed approach to solve (P2) is summarized in **Algorithm 1**.

B. Transformation of the Objective Function

By adopting the nonlinear fractional programming method [12], the following result is obtained: $\lambda^* = \max_{\mathcal{Z}} \{\frac{R(\mathcal{Z}) - S(\mathcal{Z}) + \omega Y(\mathcal{Z})}{G(\mathcal{Z})}\}$. The details of this method are given in **Algorithm 2**. The equivalent form of (P2) for a given λ is thus given by

$$(\mathrm{P3}): \quad \max_{\mathcal{Z}} \Big\{ R(\mathcal{Z}) - \tilde{S}(\mathcal{Z}) + \omega\,\tilde{Y}(\mathcal{Z}) - \lambda G(\mathcal{Z}) \Big\} \tag{12a}$$

$$\text{s.t.} \quad (4\mathrm{b})\text{-}(4\mathrm{d}), \tag{12b}$$

Algorithm 1 Iterative Successive Convex Approximation (SCA) Algorithm

Input: Set the number of iterations t, maximum number of iteration $T_{\max}$, and $\mathbf{V}_k^{(0)}$.
1: **repeat**
2: Calculate $\tilde{S}(\mathcal{Z})$ according to (9), and calculate $X_i(\mathcal{Z})$ according to (10) and (11)
3: Use **Algorithm 2** to obtain $\{\mathcal{Z}^t, \lambda^t\}$
4: Set $t = t + 1$
5: **until** $t = T_{\max}$
6: **Return** $\{\mathcal{Z}^*, \lambda^*\} = \{\mathcal{Z}^t, \lambda^t\}$

Algorithm 2 Iterative Dinkelbach Algorithm

Input: Set the maximum iteration number $i_{\max}$, the predefined weight factor ω, the error tolerance $\epsilon = 10^{-2}$, $i = 0$, and $\lambda^i = 0$.
1: **repeat**
2: Solve problem (P2) for a given λ^i and obtain $\{\mathcal{Z}^i\}$.
3: **if** $|R(\mathcal{Z}^i) - S(\mathcal{Z}^i) + \omega\, Y(\mathcal{Z}^i) - \lambda^i G(\mathcal{Z}^i)| \le \epsilon$ **then**
4: **return** $\{\mathcal{Z}^*\}$=$\{\mathcal{Z}^i\}$ and $\lambda^* = \frac{R(\mathcal{Z}^i) - S(\mathcal{Z}^i) + \omega\, Y(\mathcal{Z}^i)}{G(\mathcal{Z}^i)}$.
5: **else**
6: Set $\lambda^{i+1} = \frac{R(\mathcal{Z}^i) - S(\mathcal{Z}^i) + \omega\, Y(\mathcal{Z}^i)}{G(\mathcal{Z}^i)}$.
7: **end if**
8: **until** $i = i_{\max}$.

where $\tilde{Y}$ is obtained by (7) via substituting (11) in (10). The transformed problem (P3) is a standard semi-definite programming (SDP) which can be solved efficiently by using CVX [13].

Proposition 1: Assuming that all channel links are statistically independent, then $\mathbf{V}_k^*$ satisfies $\mathrm{Rank}(\mathbf{V}_k^*) = 1$, $\forall k$ (thus, the rank constraint in (4d) is removed without loss of optimality).

Proof: The proof can be obtained directly from [14].

C. Manifold Optimization

Last, we design the phase shifts at the IRS with the given solutions $\{\mathbf{V}_k^*, \rho_k^*, \lambda^*\}$. Note that, constraint (3d) constitutes unit-module constraints that make the problem challenging to be solved. Let us define $\mathbf{x} = [e^{j\theta_1}, \ldots, e^{j\theta_N}]^H$, $\bar{}_k = \mathrm{diag}(\mathbf{h}_{ru,k}^H)\mathbf{H}$, $\boldsymbol{\phi}_{i,k} = \bar{}_k\mathbf{v}_i$, and $\mu_{i,k} = \mathbf{h}_{bu,k}^H\mathbf{v}_i$. By this transformation, the SINR and harvested power can be represented as

$$\mathrm{SINR}_k = \frac{|\mathbf{x}^H\boldsymbol{\phi}_{k,k} + \mu_{k,k}|^2}{\sum\limits_{i\in\mathcal{K}, i\neq k} |\mathbf{x}^H\boldsymbol{\phi}_{i,k} + \mu_{i,k}|^2 + \sigma_k^2 + \frac{\delta_k^2}{1-\rho_k}}, \ \forall k, \tag{13}$$

$$\mathrm{EH} \triangleq \sum_{k\in\mathcal{K}} P_k = \sum_{k\in\mathcal{K}} \eta_k\rho_k \left(\sum_{i\in\mathcal{K}} |\mathbf{x}^H\boldsymbol{\phi}_{i,k} + \mu_{i,k}|^2 \right). \tag{14}$$

Accordingly, the optimization problem can be reformulated as

$$(\mathrm{P4}): \quad \max_{\mathbf{x}} \sum_{k\in\mathcal{K}} \log_2(1 + \mathrm{SINR}_k) + \omega\,\mathrm{EH} \tag{15a}$$

$$\text{s.t.} \quad [\mathbf{x}\mathbf{x}^{\mathrm{H}}]_{n,n} = 1, \ \forall n. \tag{15b}$$

Problem $(\mathrm{P4})$ is still non-convex due to unit-modulus constraints (15b) and the interference term in the rate objective function. To tackle this issue, we adopt a manifold optimization approach to obtain a suboptimal solution. For

this purpose, the unit-modulus constraint is handled directly by exploiting the manifold optimization theory. It should be noted that constraint (15b) specifies an oblique manifold which is expressed as [6], [15]

$$\mathcal{Q} = \{\mathbf{x} \in \mathbb{C} \mid [\mathbf{x}\mathbf{x}^{\mathrm{H}}]_{n,n} = 1, \forall\ n \in \mathcal{N}\}, \tag{16}$$

where $\mathcal{Q}$ is a Riemannian manifold. We can conclude that (15b) will be satisfied if $\mathbf{x}$ is optimized over the oblique manifold. Let us present some definitions commonly used in Riemannian manifold optimization [16]. The tangent space for $\mathcal{Q}$ at $\mathbf{x}$ can be written as

$$T_{\mathbf{x}_j}\mathcal{Q} = \{\mathbf{w} \in \mathbb{C} \mid [\mathbf{w}\mathbf{x}_j^{\mathrm{H}}]_{n,n} = 0\}, \tag{17}$$

where $\mathbf{w}$ is a tangent vector at $\mathbf{x}_j$. Let us define the objective function as the DC, i.e., $f \triangleq F + w\,\mathrm{EH} - G$, where

$$F = \sum_{k\in\mathcal{K}} \log_2\left(\sum_{i\in\mathcal{K}} |\mathbf{x}^H \boldsymbol{\phi}_{i,k} + \mu_{i,k}|^2 + \sigma_k^2 + \frac{\delta_k^2}{1-\rho_k}\right), \tag{18}$$

$$G = \sum_{k\in\mathcal{K}} \log_2\left(\sum_{i\in\mathcal{K}, i\neq k} |\mathbf{x}^H \boldsymbol{\phi}_{i,k} + \mu_{i,k}|^2 + \sigma_k^2 + \frac{\delta_k^2}{1-\rho_k}\right). \tag{19}$$

As such, the Riemannian gradient of function f at point $\mathbf{x}_j$ can be calculated based on the Euclidean gradient $\nabla_{\mathbf{x}_j} f$ onto tangent space $T_{\mathbf{x}_j}\mathcal{Q}$ that is given by

$$\mathrm{grad}_{\mathbf{x}_j} f = 2 \cdot \nabla_{\mathbf{x}_j} f - \Re\{\nabla_{\mathbf{x}_j} f \circ (\mathbf{x}_j^T)^{\mathrm{H}}\} \circ \mathbf{x}_j, \tag{20}$$

where $\nabla_{\mathbf{x}_j} f$ is established as

$$\begin{aligned}\nabla_{\mathbf{x}_j} f = \sum_{k\in\mathcal{K}} & \frac{\sum\limits_{i\in\mathcal{K}} \boldsymbol{\phi}_{i,k}\boldsymbol{\phi}_{i,k}^H \mathbf{x}_j + \sum\limits_{i\in\mathcal{K}} \boldsymbol{\phi}_{i,k}\mu_{i,k}^*}{\ln(2)\left(\sum\limits_{i\in\mathcal{K}} |\mathbf{x}_j^H \boldsymbol{\phi}_{i,k} + \mu_{i,k}|^2 + \sigma_k^2 + \frac{\delta_k^2}{1-\rho_k}\right)} \\ & + w \sum_{k\in\mathcal{K}} \sum_{i\in\mathcal{K}} \eta_k \rho_k (\boldsymbol{\phi}_{i,k}\boldsymbol{\phi}_{i,k}^H \mathbf{x}_j + \boldsymbol{\phi}_{i,k}\mu_{i,k}^*) \\ & - \sum_{k\in\mathcal{K}} \frac{\sum\limits_{i\in\mathcal{K}, i\neq k} \boldsymbol{\phi}_{i,k}\boldsymbol{\phi}_{i,k}^H \mathbf{x}_j + \sum\limits_{i\in\mathcal{K}, i\neq k} \boldsymbol{\phi}_{i,k}\mu_{i,k}^*}{\ln(2)\left(\sum\limits_{i\in\mathcal{K}, i\neq k} |\mathbf{x}_j^H \boldsymbol{\phi}_{i,k} + \mu_{i,k}|^2 + \sigma_k^2 + \frac{\delta_k^2}{1-\rho_k}\right)}.\end{aligned} \tag{21}$$

Now, we apply the conjugate gradient approach to tackle manifold optimization problems and find a (local) maximum of the function f. Consequently, the update rule of search direction in Euclidean space can be described as follows

$$\boldsymbol{\nu}_{j+1} = -\nabla_{\mathbf{x}_{j+1}} f + \alpha_j \boldsymbol{\nu}_j, \tag{22}$$

where $\boldsymbol{\nu}_j$ indicates the search direction that can be updated as Polak-Ribiere parameter to attain fast convergence [16]. Next, we introduce transport to map $\boldsymbol{\nu}_j$ from tangent space $T_{\mathbf{x}_j}\mathcal{Q}$ to tangent space $T_{\mathbf{x}_{j+1}}\mathcal{Q}$. Specifically, the vector transport for oblique manifold is expressed as

$$\begin{aligned}\mathcal{T}_{\mathbf{x}_j \to \mathbf{x}_{j+1}}(\boldsymbol{\nu}_j) \triangleq\ & T_{\mathbf{x}_j}\mathcal{Q} \to T_{\mathbf{x}_{j+1}}\mathcal{Q}: \\ & \boldsymbol{\nu_j} \to \boldsymbol{\nu_j} - \Re\{\boldsymbol{\nu_j} \circ (\mathbf{x}_{j+1}^T)^{\mathrm{H}}\} \circ \mathbf{x}_{j+1}.\end{aligned} \tag{23}$$

The search direction of the Riemannian gradient for (20) is then updated as

$$\boldsymbol{\nu_{j+1}} = -\,\mathrm{grad}_{\mathbf{x}_{j+1}} f + \alpha_j \mathcal{T}_{\mathbf{x}_j \to \mathbf{x}_{j+1}}(\boldsymbol{\nu}_j). \tag{24}$$

Algorithm 3 Manifold Optimization

Input: Set $J = 1$ as the iteration index, step size β_j, error tolerance $\xi = 10^{-2}$, $i = 0$, and $\mathbf{x}_1$ as an initial point.

1: Find the Riemannian gradient according to (20)
2: **repeat**
3: Select an appropriate β_j based on [16]
4: Calculate $\mathbf{x}_{j+1}$ via retraction in (25)
5: Update Riemannian gradient $\mathrm{grad}_{\mathbf{x}_{j+1}} f$ based on (20)
6: Compute vector transport $\mathcal{T}_{\mathbf{x}_j \to \mathbf{x}_{j+1}}(\boldsymbol{\nu}_j)$ via (23)
7: Select an appropriate Polak-Ribiere parameter based on α [16], and compute $\boldsymbol{\nu_{j+1}}$ via (24)
8: Set $j = j + 1$
9: **until** $\|\mathrm{grad}_{\mathbf{x}_j} f\| \leq \xi$.
10: Set $\hat{} = \mathrm{diag}((\mathbf{x}_{j+1}^T)^{\mathrm{H}})$

Next, we adopt retraction to find the destination on the manifold as follows

$$\mathcal{R}_{\mathbf{x}_j}(\beta_j \boldsymbol{\nu_j}) \triangleq T_{\mathbf{x}_j}\mathcal{Q} \to \mathcal{Q} : \beta_j \boldsymbol{\nu_j} \to \mathrm{unt}(\beta_j \boldsymbol{\nu_j}), \tag{25}$$

where β_j is the step size. The solution based on the above technique is summarized in **Algorithm 3**. The final AO algorithm is implemented to solve PBV and ABVs plus PS ratios alternately [5].

V. Simulation Results

In this section, numerical results are presented to assess the performance of the proposed algorithm. A two-dimensional (2D) coordinate system is considered by adopting an uniform linear array and uniform rectangular array at the BS and the IRS, respectively. All users are randomly located in the given area. The cell radius, the BS location, and the IRS location are considered as 10m, (5m, 0m) and (0m, 10m), respectively. The number of users and antennas at the BS are set to $K = 4$ and $M = 5$, respectively. All channel links are supposed to be independent Rician fading with Rician factor 10 dB and the path loss exponent is set to 2.8. The noise power at the ID, σ_k^2 and the additional noise power at the ID, δ_k^2 are set to -100 dBm and -90 dBm, respectively. The circuit power of each user p_k^{Cir}, dynamic power per reflecting component, P_{Dyn}, static power of the IRS, P_{Sta}, and the circuit power of BS, $P_{\mathrm{BS}}^{\mathrm{Cir}}$ are set to 5 mW, 0.33 mW, 100 mW, and 1 W, respectively. Moreover, the predefined non-negative weight factor ω is set to 10^5. For comparison, two benchmark system designs are investigated, namely, i) IRS-aided SWIPT with SDR method [9]; ii) IRS-aided SWIPT with random phase shifts at the IRS.

In Figs. 1 and 2, the EE for information transmission (IT) and EE for energy transmission (ET) are sketched for different system designs versus the maximum allowed transmitting power of the BS with $N = 15$. Especially, the EE for IT (EEIT) of all system designs first grows monotonically by increasing maximum transmit power and then reaches to a maximum value. This is mainly because the interference dominates over the noise for a sufficiently large value of transmit power, which results in the degradation of the EEIT of the system. Once the maximum EEIT of the system is obtained, a further increase in the transmit power would return a degradation in EEIT of the system. In contrast, it can be observed from Fig. 2 that the EE for energy transmission (EEET) grows slowly in the low transmit power region but increases quickly in the high transmit power region. Since the EEET is dominated by

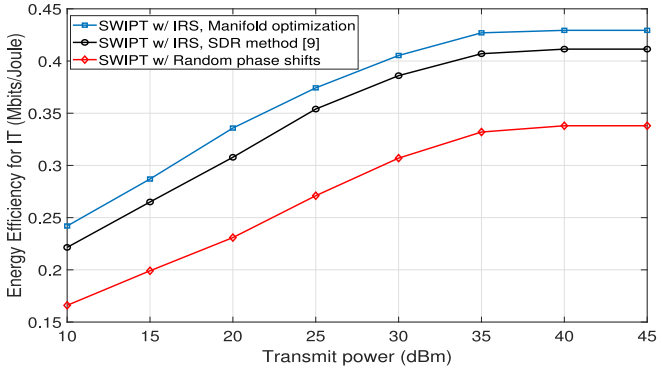

Fig. 1. EE for IT versus maximum transmit power of BS.

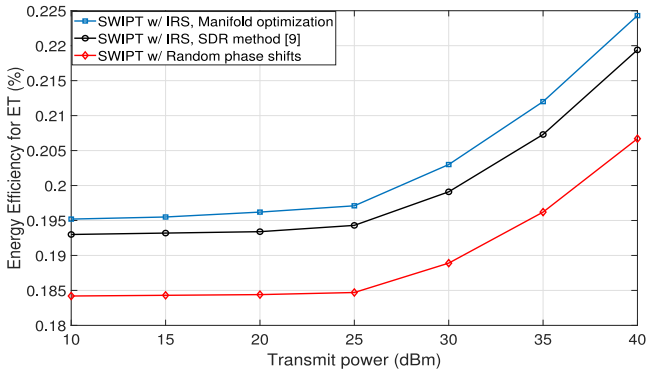

Fig. 2. EE for ET versus maximum transmit power of BS.

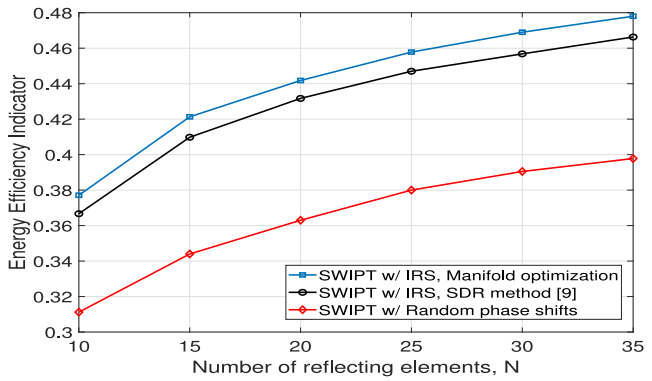

Fig. 3. EEI versus number of reflecting elements, N.

the fixed circuit power dissipation for a small transmit power which gives rise to a slowly increasing rate of EEET with the transmit power. However, for higher values of the transmit power, the resulting intensified interference limits the maximum achievable data rate of users to a system-dependent value which in return results in a saturated EEIT value of the system. Also, it is observed that the obtained EEIT and EEET with the proposed manifold optimization-based algorithm is superior over the benchmarks since our proposed algorithm yields a locally optimal solution, while the SDR approach provides only an approximate solution. Besides, the random phase shifts deteriorate the system performance drastically in terms of EEIT and EEET.

Fig. 3 depicts the EEI versus the number of reflecting elements, N, for different schemes, while keeping the maximum transmit power as $P_{max} = 35$ dBm. As observed, all schemes show the same increasing trend of EEI with larger, N. This is because increasing N results in much higher SE but only moderately increased total power consumption, which leads to higher EEI.

VI. Conclusion

In this letter, we investigated the joint design of ABVs at the BS and PBV at the IRS for a multiuser MISO IRS-aided SWIPT system with the PS-based receiver. Specifically, the EEI was introduced to strike a balance between the EEs of data transmission and energy transfer and optimized subject to the maximum transmit power budget at the BS. To solve this problem, we adopted the AO, SDR, MM, and Dinkelbach techniques. In particular, a novel manifold approach was proposed to design the phase shifts at the IRS under their unit-modulus constraints. Simulation results demonstrated the effectiveness of the new manifold approach and the performance gains of the proposed algorithm as compared to various benchmarks. In future work, this letter can be extended to the practical case with imperfect CSI which requires robust beamforming design.

References

[1] Q. Wu, S. Zhang, B. Zheng, C. You, and R. Zhang, "Intelligent reflecting surface aided wireless communications: A tutorial," 2020. [Online]. Available: https://arxiv.org/abs/2007.02759.

[2] Q. Wu and R. Zhang, "Towards smart and reconfigurable environment: Intelligent reflecting surface aided wireless networks," *IEEE Commun. Mag.*, vol. 58, no. 1, pp. 106–112, Jan. 2020.

[3] Q. Wu and R. Zhang, "Beamforming optimization for wireless network aided by intelligent reflecting surface with discrete phase shifts," *IEEE Trans. Commun.*, vol. 68, no. 3, pp. 1838–1851, Mar. 2020

[4] C. Pan *et al.*, "Multicell MIMO communications relying on intelligent reflecting surfaces," *IEEE Trans. Wireless Commun.*, vol. 19, no. 8, pp. 5218–5233, Aug. 2020.

[5] Z. Yang *et al.*, "Energy-efficient wireless communications with distributed reconfigurable intelligent surfaces," [Online]. Available: https://arxiv.org/abs/2005.00269.

[6] H. Guo, Y.-C. Liang, J. Chen, and E. G. Larsson, "Weighted sum-rate maximization for reconfigurable intelligent surface aided wireless networks," *IEEE Trans. Wireless Commun.*, vol. 19, no. 5, pp. 3064–3076, May. 2020.

[7] Y. Zeng, B. Clerckx, and R. Zhang, "Communications and signals design for wireless power transmission," *IEEE Trans. Commun.*, vol. 65, no. 5, pp. 2264–2290, May 2017.

[8] B. Clerckx, R. Zhang, R. Schober, D. W. K. Ng, D. I. Kim, and H. V. Poor, "Fundamentals of wireless information and power transfer: From RF energy harvester models to signal and system designs," *IEEE J. Sel. Areas Commun.*, vol. 37, no. 1, pp. 4–33, Jan. 2019.

[9] Q. Wu and R. Zhang, "Weighted sum power maximization for intelligent reflecting surface aided SWIPT," *IEEE Wireless Commun. Lett.*, vol. 9, no. 5, pp. 586–590, May 2020.

[10] Q. Wu and R. Zhang, "Joint active and passive beamforming optimization for intelligent reflecting surface assisted SWIPT under QoS constraints," *IEEE J. Sel. Areas Commun.*, vol. 38, no. 8, pp. 1735–1748, Aug. 2020

[11] C. Pan *et al.*, "Intelligent reflecting surface aided MIMO broadcasting for simultaneous wireless information and power transfer," *IEEE J. Sel. Areas Commun.*, vol. 38, no. 8, pp. 1719–1734, Aug. 2020.

[12] W. Dinkelbach, "On nonlinear fractional programming," *Manag. Sci.*, vol. 13, no. 7, pp. 492–498, Mar. 1967.

[13] M. Grant and S. Boyd. *CVX: MATLAB Software for Disciplined Convex Programming*. Accessed: Mar. 2014. [Online]. Available: http:cvxr.com/cvx

[14] Q. Shi, L. Liu, W. Xu, and R. Zhang, "Joint transmit beamforming and receive power splitting for MISO SWIPT systems," *IEEE Trans. Wireless Commun.*, vol. 13, no. 6, pp. 3269–3280, Jun. 2014.

[15] X. Yu, D. Xu, and R. Schober, "MISO wireless communication systems via intelligent reflecting surfaces," in *Proc. IEEE ICCC*, Changchun, China, Aug. 2019, pp. 735–740.

[16] P.-A. Absil, R. Mahony, and R. Sepulchre, *Optimization Algorithms on Matrix Manifolds*. Princeton, NJ, USA: Princeton Univ. Press, 2009.